Neutron scattering studies of polymers in supercritical carbon dioxide

1999 J. Phys.: Condens. Matter 11 R157

(http://iopscience.iop.org/0953-8984/11/15/006)

J. Phys.: Condens. Matter **11** (1999) R157–R177. Printed in the UK PII: S0953-8984(99)88540-3

REVIEW ARTICLE

Neutron scattering studies of polymers in supercritical carbon dioxide

George D Wignall

Solid State Division, Oak Ridge National Laboratory†, Oak Ridge, TN 37831-6393, USA

Received 4 December 1998

Abstract. Above its critical point, carbon dioxide forms a supercritical fluid (SCF) that promises to be an environmentally responsible replacement for the organic solvents currently used in polymer synthesis and processing. Over the past two decades, small-angle neutron scattering (SANS) has provided a wealth of novel structural information on polymers and, more recently, the technique has been applied to characterize molecules dissolved in CO_2 (e.g. fluoropolymers and siloxanes). When the interactions between the chain segments and the surrounding fluid are balanced, the chain trajectory is independent of both segment–segment and solvent–solute interactions. This phenomenon occurs at a 'theta temperature' (T_θ), where chain dimensions correspond to a volumeless polymer coil, 'unperturbed' by long range interactions. For $T > T_\theta$, the system exhibits a 'good solvent' domain, where the molecules expand beyond the unperturbed R_g in both organic solvents and in CO_2. However, unlike organic solvents, this transition can be made to occur at a critical 'theta pressure' (P_θ) in CO_2 and this represents a new concept in the physics of polymer–solvent systems. For $T < T_\theta$, and $P < P_\theta$, the system enters the 'poor solvent' domain, where diverging concentration fluctuations prevent the chains from collapsing and allow them to maintain their unperturbed dimensions.

Other polymers such as polystyrene (PS) are insoluble in CO_2, though they may be solubilized by means of PS-fluoropolymer stabilizers, which function as surfactants. In the case of such diblock-copolymers, aggregation occurs when the solvent is preferential for one of the blocks and SANS may be used to determine the structure of the aggregates (micelles), which consist of a CO_2-phobic core surrounded by a CO_2-philic shell. When CO_2-insoluble material (e.g. PS) is added to the block-copolymer solutions, virtually all of the material is solubilized in the core.

A unique attribute of SCFs is that the solvent quality may be adjusted over a wide range by varying the density (pressure), thus offering significant control over the solubility. This paper will illustrate the use of a tunable solvent to control the quality of the solvent–solute interaction of homopolymers and the self assembly of block-copolymer surfactants. SANS promises to give the same level of insight into polymers and amphiphiles in supercritical media that it has provided in the condensed state, organic solvents and in aqueous systems.

1. Introduction

Carbon dioxide is nontoxic, nonflammable, naturally occurring, recyclable and inexpensive. Above its critical pressure ($P_c = 72$ bar) and temperature ($T_c = 31\,^\circ$C), CO_2 has properties intermediate between a gas and a liquid, i.e. high density and low viscosity. Because of these attributes, supercritical CO_2 has been proposed as an environmentally responsible replacement for the organic solvents used in many industrial applications. However, only two classes of polymeric materials (amorphous fluoropolymers and silicones) have been shown [1–4] to exhibit appreciable solubility in CO_2 at readily accessible temperatures and pressures

† Operated by Lockheed Martin Energy Research Corporation under contract No DE-AC05-96OR22464 for the US Department of Energy.

($T \sim 100\,^{\circ}$C, $P \sim 500$ bar). Thus, many polymers (e.g. long-chain hydrocarbons, waxes, heavy greases etc) do not dissolve in CO_2 and this necessitates the use of emulsifying agents to solubilize the 'CO_2-phobic' material. Such surfactants are generally amphiphilic (i.e. the different components of the molecule have different solubilities), and it is well known that hydrophobic oil may be solubilized in water by coating the oil droplets with the hydrophilic (water-soluble) component of a detergent.

The first successful dispersion polymerization in super-critical CO_2 involved the stabilization of poly(methyl methacrylate) (PMMA) particles [1] by the homopolymer poly(1,1-dihydroperfluoro-octylacrylate) (PFOA), which coated the PMMA particles with 'CO_2-philic' fluorinated side chains, and were anchored by the acrylic groups in the backbone. In order to allow the synthesis of other polymers (e.g. polystyrene), diblock-copolymers have been synthesized for use as emulsifying agents in heterogeneous polymerizations by DeSimone and co-workers [5–8]. Because of their amphiphilic character, these molecules form micelles, which stabilize the polymerization of styrene in CO_2 and give rise to spherical particles in quantitative ($>$90%) yields [2]. Subsequently, molecularly engineered diblock-copolymer surfactants, consisting of 'CO_2-phobic' and 'CO_2-philic' blocks, have been developed [5] for a wide range of applications in liquid and supercritical CO_2. These include the stabilization of polymer colloids during dispersion polymerizations [6–8], the formation of micelles [5] which can solubilize CO_2-insoluble substances [9] and liquid–liquid extractions via the phase transfer of water-soluble substances from water into a surfactant-rich liquid CO_2 phase [10].

Small-angle neutron and x-ray scattering (SANS and SAXS) methods allow the elucidation of the size and shape of both single polymer chains [11, 12] and supramolecular structures [13, 14], in the resolution range 5–2000 Å. SAXS and light scattering (LS) have been applied since the 1940s to provide structural information on polymer solutions, though the limit of zero concentration was required to eliminate interchain interference. Thus, these methods could not be applied to the condensed state or to concentrated solutions, due to the difficulties of separating the *inter*- and *intra*-chain contributions to the structure. However, SANS has removed this limitation and due to a fortuitous combination of several factors: high bulk penetrating power, the ability to manipulate local scattering amplitudes through isotopic labelling or an appropriate choice of solvent (contrast variation), the technique has developed into an extremely powerful tool for the study of polymers. By deuterating a fraction of the polymer, it is possible to measure the single-chain structure factor and thus the R_g of the polymer chains in concentrated solvents [15–17], and high-concentration labelling methods have been developed to maximize the signal-to-noise of such experiments [18]. Thus, over the past two decades, SANS has been widely applied to study polymer solutions and the self-assembly of amphiphiles in aqueous media [13, 14, 19]. More recently, the technique has been used to study polymers in CO_2 [3–5, 9, 20–25] and other gases [26, 27] and it is particularly suited to study the structure of fluids under pressure [28, 29], due to the high transmission of many of the materials used in the construction of pressure vessels. However, SAXS [10, 30, 31] and LS [32] experiments highlight different components of the structure and thus complement the information from SANS, though the development of a SAXS high-pressure cell is a more challenging task than for SANS [2, 6, 7] or LS [33]. This publication will focus on SANS studies of both CO_2-soluble homopolymers and also the micellar structures formed by amphiphilic block-copolymer surfactants.

2. Experiment

Most of the SANS data described in this article were collected on the W C Koehler 30 m SANS facility [34] at the Oak Ridge National Laboratory (ORNL) or on comparable facilities that

probe a similar range of dimensions. The neutron wavelength was $\lambda = 4.75$ Å ($\Delta\lambda/\lambda \sim 5\%$) and the 64×64 cm^2 area detector with cell size $\sim$1 cm^2 was placed at various sample–detector distances (3–10 m). The data were corrected for instrumental backgrounds and detector efficiency on a cell-by-cell basis, prior to radial (azimuthal) averaging, to give a Q-range of $0.006 < Q = 4\pi\lambda^{-1}\sin\theta < 0.1$ Å^{-1}, where 2θ is the angle of scatter. The net intensities were converted to an absolute ($\pm$3%) differential cross-section per unit solid angle, per unit sample volume ($\mathrm{d}\Sigma(Q)/\mathrm{d}\Omega$ in units of cm^{-1}) by comparison with pre-calibrated secondary standards [35]. The experiments were conducted in the same cell that has been used for polymer synthesis [2, 6, 7] and, due to the high penetrating power of neutrons, the beam passed through two 1 cm sapphire windows, with virtually no attenuation (cell transmission $\simeq$93%) or parasitic scattering. The sample cross sections were obtained by subtracting the intensities of the empty cell with sapphire windows. The signal of the cell filled only with CO_2 amounted to a virtually flat background ($\sim$0.04 cm^{-1}), which formed only a minor correction to the scattering from the homopolymer and block-copolymer solutions.

Cross-calibration experiments were performed on the ORNL 10 m SAXS instrument [36, 37], with a sample–detector distance of 5.1 m using Cu Kα radiation ($\lambda = 1.54$ Å) and a 20×20 cm^2 area detector with cell (element) size $\sim$3 mm. Corrections for instrumental backgrounds and detector efficiency have been described previously [9, 36, 37] and the net intensities were radially averaged in the Q-range $0.009 < Q < 0.055$ Å^{-1} before conversion to an absolute differential cross section by means of pre-calibrated secondary standards [38]. The monoblock stainless steel SAXS cell was similar to that described earlier by Fulton and co-workers [30, 31, 39] and comprised two ports for the single-crystal diamond windows (1 mm total thickness), a sapphire view port, used to verify phase homogeneity, and the gas injection port. The x-ray path length was $\simeq$0.5 mm.

3. Results and discussion: CO_2-soluble polymers

For a homogenous polymer solution the methodology to extract the R_g, the radius of gyration (i.e. the r.m.s. distance of scattering elements from the centre of gravity) and the second virial coefficient (A_2), which indicates whether a polymer chain swells or contracts in the presence of a solvent, is well established [3, 4, 40]. These parameters are related to the cross-section via

$$Kc\left[\frac{\mathrm{d}\Sigma}{\mathrm{d}\Omega}(0)\right]^{-1} \simeq \frac{1}{M_w} + 2A_2c \tag{1}$$

where A_2 is the second virial coefficient, c is the concentration (g cm^{-3}), M_w is the (weight-averaged) molecular weight, A_0 is Avogadro's number and $K = [\Delta(\mathrm{SLD})]^2/\rho_p^2 A_0$ is the contrast factor. ρ_p is the polymer density and it has been assumed that the volume from which CO_2 is excluded by a polymer segment in the supercritical fluid is the same as the molecular volume in the solid state. The scattering length density (SLD) is defined as the sum of coherent scattering lengths over all atoms lying in a given volume ΔV, divided by ΔV [12], and Δ(SLD) is the difference between the values for the polymer (0.0336×10^{12} cm^{-2} for PFOA) and CO_2 ($2.498\rho_{CO_2} \times 10^{10}$ cm^{-2}). This gives $K = 7.5 \times 10^{-5}$ mol cm^2 g^{-2} for PFOA at $T = 65\,^\circ$C and $P = 340$ bar, where SANS was used [4] to measure A_2 and M_w in the ranges $0.6 < 10^4 A_2 < 0.25$ and $114 < 10^{-3} M_w < 1000$. The molecular structure of PFOA is indicated in figure 1 and the R_g was derived from the measured cross-sections using both Zimm plots (for the low-Q data points) and also by fitting the data to a Debye random coil model [11, 12], with good agreement ($\pm$5%) between the two approaches (figure 1). As the pressure is reduced, the solubility decreases and the PFOA falls out of solution at the critical,

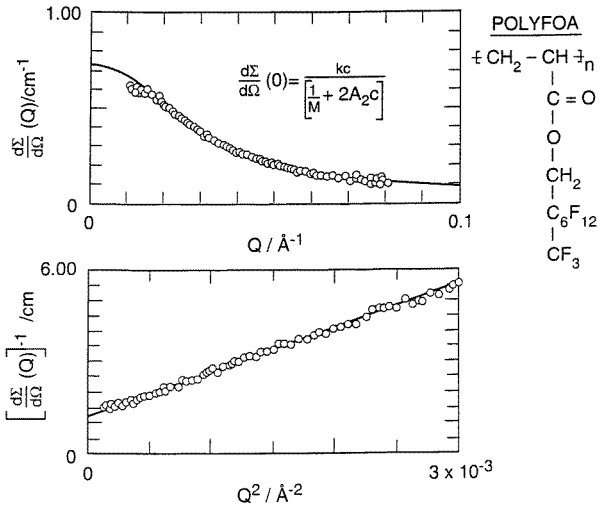

Figure 1. Zimm and Debye fits to SANS data for 10% (w/v) high-molecular-weight PFOA in supercritical CO_2. (Reprinted from D Chillura-Martino *et al* 1996 Neutron scattering characterization of polymerization mechanisms in supercritical CO_2 *J. Mol. Struct.* **383** with permission from Elsevier Science.)

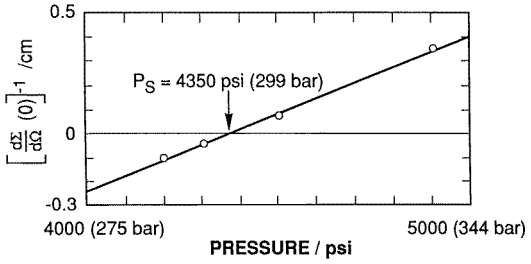

Figure 2. Solubility determination using SANS for 3% (w/v) PFOA in CO_2 at 65 °C. (Reprinted from D Chillura-Martino *et al* 1996 Neutron scattering characterization of polymerization mechanisms in supercritical CO_2 *J. Mol. Struct.* **383** with permission from Elsevier Science.)

'neutron cloud point' ($T = 65\,^{\circ}$C, $P \simeq 300$ bar), as indicated (figure 2) by a zero intercept on the ordinate ($\mathrm{d}\Sigma/\mathrm{d}\Omega(0) \rightarrow \infty$).

The chain dimensions are a function of the (weight-averaged) molecular weight (M_w) and may be summarized as $R_g = (0.10 \pm 0.02) M_w^{0.5}$. The second virial coefficient (A_2) is positive and decreases with molecular weight, as is generally observed for polymer solutions, where $A_2(M_w)$ is empirically described by $A_2 \sim M_w^{-\delta}$, with $\delta \simeq 0.3$ in various systems [41]. From the two data points in table 1 the exponent is $\delta = 0.4$ for PFOA in supercritical CO_2, showing that the variation of A_2 with M_w is reasonable, as the error in δ is ± 0.1. These results indicate that transport of monomers to the inside of the PFOA chains or aggregates would occur more efficiently for the low-M_w polymer, for which A_2 is larger and hence the chains are more swollen as the molecular weight decreases.

Figure 3 shows a plot of $Kc[\mathrm{d}\Sigma/\mathrm{d}\Omega(0)]^{-1}$ against c for hexafluoropropylene oxide (HFPPO) or Krytox^{TM} and the values of A_2 and M_w are compared to the equivalent quantities for PFOA in table 1. The magnitude of M_w measured by SANS is in good agreement with

Table 1. Molecular weight (M_w), second virial coefficient (A_2), radius of gyration (R_g) and $R_g/M_w^{1/2}$ for PFOA and hexafluoropropylene oxide (HFPPO).

Polymer	$10^{-3}M$ (g mol^{-1})	$10^4 A_2$ (cm^3 g^{-2} mol)	R_g (Å)	$R_g/M_w^{1/2}$ (Å g$^{-0.5}$)
HMW-PFOA	1000 ± 400	0.25 ± 0.05	100 ± 9	0.10 ± 0.02
LMW-PFOA	110 ± 20	0.6 ± 0.1	34 ± 5	0.10 ± 0.02
HFPPO	13 ± 1	0.0 ± 0.2	26–33	~0.24

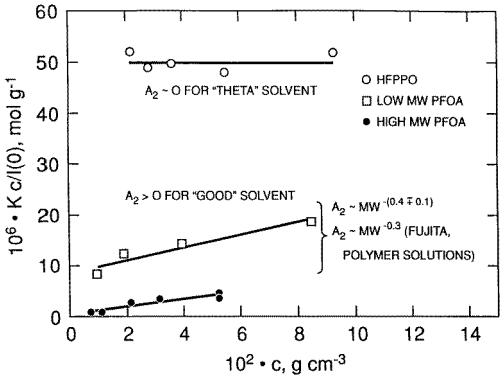

Figure 3. PFOA and HFPPO (Krytox^{TM}) in CO_2 at 5000 psi (344 bar) and 65 °C.

the nominal M_w given by the manufacturer (16 k) and A_2 is zero within the experimental error. For $0.02 < c < 0.093$ g cm^{-2}, values of R_g are in the range 26–33 Å, giving $R_g/M_w^{0.5} \sim 0.24$ Å (g mol)$^{-0.5}$, compared to 0.45 for polyethylene, 0.35 for polypropylene and 0.1 Å (g mol)$^{-0.5}$ for PFOA. Thus, polyethylene molecules have the largest size for a given M_w, because all the CH_2 groups are in the backbone. As the fraction of the groups in the pendant group increases, the size of the coil for a given molecular weight becomes smaller as the fraction of the segment in the chain backbone decreases. The first experiments on polydimethylsiloxane (PDMS) in CO_2 were undertaken by Chillura-Martino *et al* [4] and figure 4 shows $Kc[d\Sigma/d\Omega(0)]^{-1}$ against concentration at $T = 65\,^{\circ}$C and $P = 344$ bar. Above $c \simeq 0.02$ g cm^{-3}, both $d\Sigma/d\Omega(0)$ and R_g increase disproportionately with concentration and similar behaviour is exhibited at $T = 40\,^{\circ}$C. Thus, the slope of the plot and hence the second virial coefficient derived from it, is negative.

In organic solvents, it is well known that the dimensions of polymer molecules depend on the sign and magnitude of the interactions between the chain segments and the molecules of the surrounding liquid. In 'good' solvents, the *intra*-chain repulsion or excluded volume between the segments works to expand R_g, as does the solvent–solute interaction and A_2 is positive. In less favourable solvents, however, the solvent–solute and solute–solute interactions have opposite signs, and, when they are balanced, the chain dimensions are independent of both segment–segment and solvent–solute interactions. This phenomenon occurs at the Flory or 'theta temperature' (T_θ), where A_2 is zero and R_g corresponds to the dimension of a volumeless polymer coil, 'unperturbed' by long-range interactions. One of the first significant applications of SANS was to confirm Flory's prediction that polymer chains would adopt such random-walk configurations in the condensed (amorphous) state [11]. In the poor solvent regime ($T < T_\theta$), the attractive and repulsive forces are no longer balanced and the second virial coefficient is

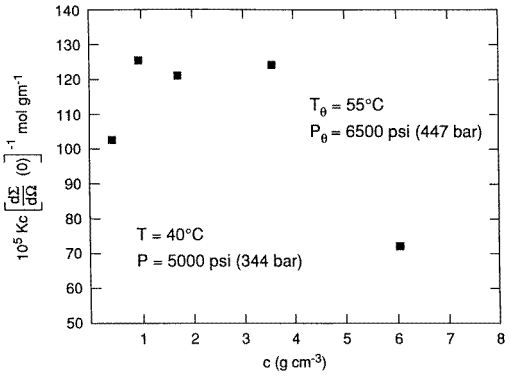

Figure 4. Inverse ($Q = 0$) cross-section as a function of the concentration of polydimethylsiloxane in CO_2. (Reprinted from D Chillura-Martino *et al* 1996 Neutron scattering characterization of polymerization mechanisms in supercritical CO_2 *J. Mol. Struct.* **383** with permission from Elsevier Science.)

negative.

This phenomenon is well understood for dilute polymer solutions, where the macromolecules are widely separated and *inter*-chain effects can be neglected [42]. SANS has recently been used to extend the experimental observations to concentrated solutions (where the chains overlap and interpenetrate) and to test current theoretical predictions. These have hitherto been based mainly on the de Gennes' concept [43] that at the critical (demixing) point (T_c), polymer chains do not interpenetrate significantly and thus are collapsed (i.e. $R_g(T_c) < R_g(T_\theta)$) as in dilute solutions. However, SANS experiments on polystyrene in cyclohexane undertaken by Melnichenko and coworkers [44, 45] have demonstrated that the predicted decrease in R_g is not observed as $T \to T_c$. As the solutions studied were close to the concentration where the molecules overlap, a fraction of the polymer was deuterated to extract the single chain R_g. For unlabelled solutions, the size of the concentration fluctuations may be measured via the Ornstein–Zernike (O–Z) formalism [12]

$$\frac{d\Sigma}{d\Omega}(Q) = \frac{d\Sigma}{d\Omega}(0)/(1 + Q^2\xi^2) \tag{2}$$

where ξ is the composition fluctuation correlation length, which may be obtained from the slope of an O–Z plot of $(d\Sigma/d\Omega(0)]^{-1}$ against Q^2. ξ diverges near T_c, where it exceeds the chain dimensions ($\xi > R_g$) and leads to the formation of distinct microdomains of interpenetrating molecules, which stabilize the dimensions and prevent the expected collapse in organic solvents [44]. So effective is this mechanism that it has been shown that, even for solutions which never leave the poor solvent domain, and cannot reach the θ-domain (e.g. polystyrene in acetone), the molecules are always 'stabilized' to exhibit the 'theta dimensions' over wide ranges of pressure and temperature [45].

SANS has also been used [46] to study the dimensions of polymer molecules in supercritical CO_2 to test the prediction [47] that they will adopt 'ideal' configurations, unperturbed by excluded volume effects, at a critical 'theta pressure' (P_θ) as they do in polymer solutions at the theta temperature. Experiments on PDMS in CO_2 (figures 5 and 6) confirm that the system exhibits both of these phenomena at a theta pressure, $P_\theta = 447$ bar and temperature $T_\theta = 55\,^\circ$C. To the author's knowledge, this is the first time that the existence of a 'theta pressure' has been demonstrated and this effect constitutes a new concept in the physics of polymer–solvent systems. It is of fundamental importance for understanding not

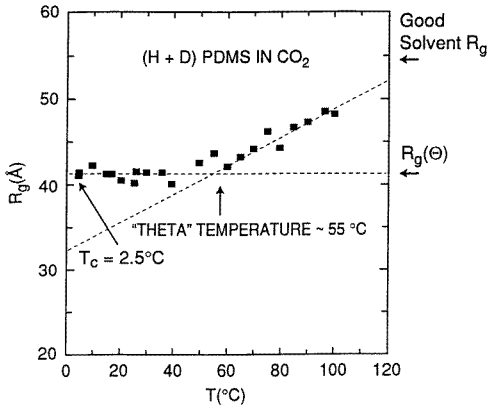

Figure 5. Expansion of polydimethylsiloxane (PDMS) in CO_2 above the 'theta temperature' ($T_\theta \sim 55\,^\circ$C). Below T_θ, diverging concentration fluctuations prevent the coil collapsing as observed in organic solvents.

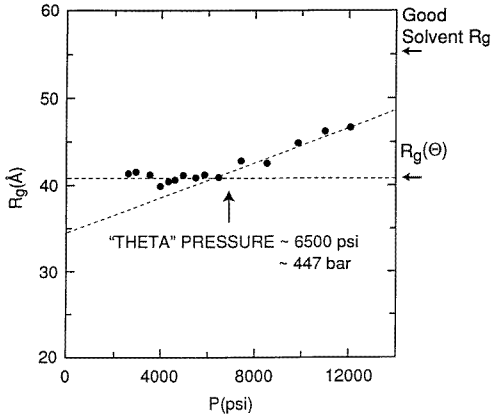

Figure 6. First observation of a 'theta pressure' in supercritical CO_2. As observed in organic solvents, the chains do not collapse below T_θ or P_θ.

only the properties of polymer solutions, but also the phase transitions of proteins in biological systems.

For $P > P_\theta$ and $T > T_\theta$, the system exhibits a 'good solvent' domain, where the polymer molecules expand beyond the unperturbed R_g, measured in the condensed (solid) state. However, for $T < T_\theta$, and $P < P_\theta$, the chains do not collapse as expected (figures 5 and 6). Instead, they maintain their unperturbed dimensions, as observed in organic solvents [44], where the size of the concentration fluctuations, ξ diverges as $T \to T_c$, the critical demixing temperature. Thus, the deterioration of the solvent quality again leads to the formation of microdomains, consisting of interpenetrating polymer coils, as in organic solvents. Near the critical point, the growth of the polymer concentration fluctuations brings together the initially diluted chains, and the molecules adopt the unperturbed dimensions, as in highly concentrated systems and in the condensed state. Thus, the stabilization of the molecular dimensions in the poor solvent domain by diverging concentration fluctuations is a universal phenomenon, observed not only in 'classical' polymer solutions (e.g. polystyrene in cyclo-hexane), but also

in supercritical fluids (e.g. PDMS in CO_2). In the light of these discoveries, it may be seen that the initial experiments on PDMS [4] were performed at temperatures and pressures $T < T_\theta$, and $P < P_\theta$, where CO_2 is a 'poor' solvent for PDMS and this is consistent with the negative slope (figure 4) and second virial coefficient. Thus, for the three 'CO_2-soluble' molecules studied at $T \sim 65\,^\circ$C and $P \sim 350$ bar, CO_2 is either a 'good' solvent (PFOA), a theta solvent (HFPPO) or a 'poor' solvent (PDMS) and there is a close similarity between the behaviour of polymer molecules in organic solvents [43–45] and in CO_2 [46, 47].

However, a unique attribute of SCFs is that the solvent strength is easily tunable with changes in the system density, offering exceptional control over the solubility. Thus, for PDMS, CO_2 becomes a 'theta' solvent at $P_\theta \sim 447$ bar and $T_\theta \sim 55\,^\circ$C, whereas it behaves as a 'good' solvent for $P > P_\theta$ and $T > T_\theta$. Below this transition, the chain dimensions never fall below the 'theta' R_g, as observed in organic solvents, though for supercritical CO_2, the system may be driven through this transition as a function of pressure in addition to temperature. Understanding the solubility mechanisms is a necessary condition for the development of CO_2-based technologies and SANS promises to give the same level of insight into polymers and amphiphiles in supercritical media that it has provided in the condensed state, organic solvents and in aqueous systems.

4. Results and discussion: CO_2-insoluble polymers

As many industrially important polymers do not dissolve in supercritical CO_2 at readily accessible temperatures ($<100\,^\circ$C) and pressures (<500 bar), this necessitates the use of solubilization techniques, which may be defined as 'the preparation of a thermodynamically stable isotropic solution of a substance normally insoluble . . . in a given solvent' [48]. Thus, the first successful dispersion polymerization in supercritical carbon dioxide [8] involved the stabilization of poly(methyl methacrylate) (PMMA) by PFOA, which were anchored via the acrylic groups in the molecule and coated the growing particles with 'CO_2-philic' fluorinated side chains. Subsequently, specifically designed 'soaps' or emulsifying agents have been developed [5]. These molecularly engineered diblock-copolymer surfactants, consisting of 'CO_2-phobic' and 'CO_2-philic' blocks, have been used for a wide range of applications in liquid and supercritical CO_2. As mentioned above, amphiphilic surfactants have been widely studied in aqueous media and have been shown to self-assemble into a range of aggregates (micelles, microemulsions etc) via SANS [13, 14, 19, 49]. The existence of micelles and microemulsions in supercritical CO_2 has been debated for a decade [50, 51] and scattering techniques have recently been applied to address this issue.

4.1. The polydisperse core–shell model and application to water-in-CO_2 microemulsions

The first small-angle scattering study of aggregation mechanisms of copolymer micelles in supercritical CO_2 was undertaken by Fulton and coworkers [31] on H_2O-swollen PFOA–polyethylene oxide (PFOA-g-PEO) graft copolymers using SAXS. The copolymer concentration was in the range 0.6–1.9% (w/w) and it was shown that core–shell micellar structures were formed with inner (R_1) and outer (R_2) radii of 105 and 125 Å respectively. A schematic illustration of the micelle is shown in figure 7 and the particles were shown to be capable of solubilizing appreciable quantities ($\sim$30% w/w of copolymer) of water into CO_2. Complementary studies of water-in-CO_2 microemulsification were undertaken by Johnston and co-workers [52], who demonstrated similar levels of water 'encapsulation' in micelles formed by ammonium carboxylate perfluoroether surfactants via spectroscopic techniques. The solubilized water was shown [52] to create an environment that closely resembled bulk

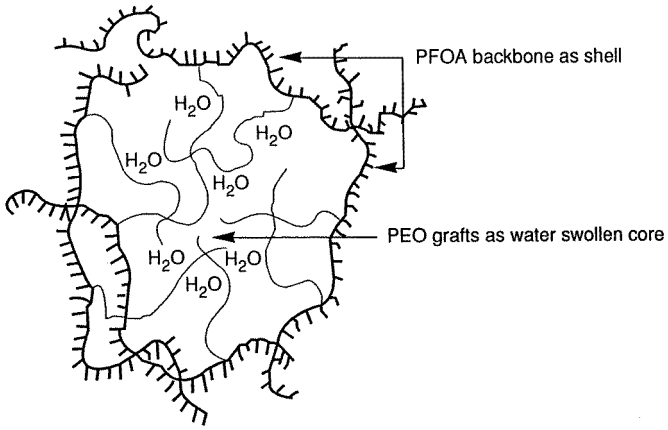

Figure 7. Schematic of PFOA-g-PEO micelle in CO_2 (from Fulton *et al* [31]). (Reprinted with permission from Fulton *et al* 1995 *Langmuir* **11** 4241. Copyright 1995 American Chemical Society.)

water. Because aggregates formed by surfactants in a predominantly water phase have been traditionally referred to as 'normal' micelles, those forming in a predominantly oil matrix are often referred to as 'reverse micelles' [23, 31, 50] or 'inverted micelles' [22]. Thus, aggregates that form in CO_2 may also be referred to as 'reverse micelles' [23, 31, 50], as the hydrophilic component is in the core, and those that are capable of absorbing appreciable amounts of water are described as water-in-CO_2 microemulsions [23, 31] by analogy with water-in-oil systems.

In the SAXS study [31], the intensities were recorded in arbitrary units and thus it was not possible to check whether the model reproduced the absolute cross-section [35, 48], in addition to the shape of the scattered intensity. Subsequently Chillura-Martino and co-workers [4] refined this study by repeating the measurements via SANS using absolute units (cm^{-1}), and taking advantage of the contrast variation opportunities afforded by substituting D_2O for H_2O. This allowed a more stringent test of the model dimensions, though it did not alter the overall conclusions of the previous study. The material was also examined in the absence of added water to show that the micelle dimensions are much smaller and to quantify the structural changes induced by water-swelling.

Figure 8 shows the dramatic differences in the SANS data introduced by H_2O- and D_2O-swelling, as the radius of gyration increases from ∼56 Å for the unswollen micelle to ∼82 Å (H_2O-swollen) and 136 Å (D_2O-swollen). The SANS data were modelled [4, 19] as a system in which core–shell micelles interact in a solvent medium. For a collection of polydisperse particles, assuming no orientational correlations the coherent differential scattering cross-section is given by

$$\frac{d\Sigma}{d\Omega}(Q) = N_p[\langle|F(Q)|^2\rangle + |\langle F(Q)\rangle|^2(S(Q) - 1)] + B \tag{3}$$

where N_p is the number density of particles, $S(Q)$ is the structure function arising from interparticle scattering and B is the coherent background from CO_2 (∼0.04 cm^{-1}). For the dilute solutions (e.g. $c < 2\%$ w/v) considered here, interparticle interactions may be neglected, and the interparticle structure function in this case is similar to that of a dilute gas ($S(Q) \simeq 1$).

Spherical particles with a centrosymmetric distribution of scattering length density may be modelled by a set of concentric shells [14, 19], and for a core–shell micelle, the intra-particle

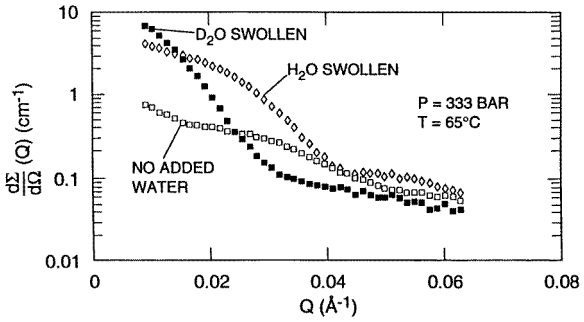

Figure 8. $d\Sigma/d\Omega(Q)$ for PFOA-g-PEO graft copolymer in CO_2, before and after swelling with D_2O. (Reprinted from D Chillura-Martino *et al* 1996 Neutron scattering characterization of polymerization mechanisms in supercritical CO_2 *J. Mol. Struct.* **383** with permission from Elsevier Science.)

term in equation (2) may be expressed as

$$\langle |F(Q)|^2 \rangle = \int |F(Q, R_1)|^2 f(R_1)\, dR_1. \tag{4}$$

R_1 is the radius of a core, which occurs within the distribution of core radii with a frequency of $f(R_1)$, and the structure function of a particle with core radius R_1 and outer radius R_2 is given by

$$F(Q, R) = \frac{4\pi}{3}\lfloor R_1^3(\rho_1 - \rho_2)F_0(QR_1) + R_2^3(\rho_2 - \rho_s)F_0(QR_2)\rfloor$$
$$F_0(x) = \frac{3}{x^3}(\sin x - x\cos x) \tag{5}$$

where ρ_1, ρ_2 are the core and shell SLDs.

Several particle shapes were used to calculate $P(Q)$, and the best fits were given by a spherical core–shell model with a Schultz distribution [19] of particle sizes

$$f(R_1) = \frac{(Z+1)^{Z+1}X^Z \exp[-(Z+1)X]}{\bar{R}_1\Gamma(Z+1)}$$
$$Z = \frac{1 - \left(\sigma/\bar{R}_1\right)^2}{\left(\sigma/\bar{R}_1\right)^2}$$
$$X = \frac{R_1}{R_2} \tag{6}$$

where σ^2 is the variance of the distribution, Z is the breadth parameter.

It was not possible to determine unequivocally the location of the aqueous species in the previous study [31], which assumed that the core (the probable location of the absorbed water) had the bulk (unswollen) PEO density. Figures 9 and 10 show fits to the SANS data using the core–shell model and changing only the contrast between the H_2O- and D_2O-swollen systems. The inner radii were $\simeq$86 Å for both the H_2O- and D_2O-swollen micelles and the outer radius was 130 Å (D_2O-swollen) and 126 Å (H_2O-swollen) respectively. The aggregation number (i.e. the number of copolymer molecules per micelle) was $N_{agg} \simeq 83$, compared to $N_{agg} \simeq 120$ derived via SAXS [31], and $N_{agg} \simeq 3$ for the unswollen micelle. Thus, the basic overall picture remains the same as in the initial study, though the extra information provided by absolute units and contrast variation methods allowed a more detailed description of the system.

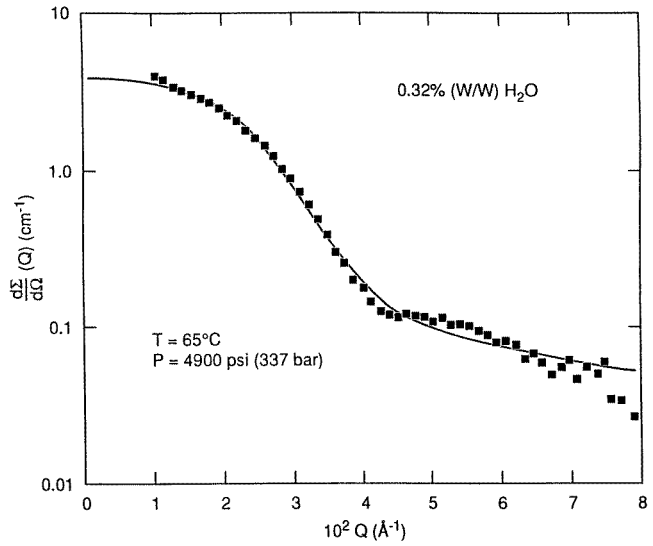

Figure 9. SANS data for 1.9% (w/v) PFOA-g-PFOA graft copolymer in H_2O-saturated CO_2 compared to the polydisperse core–shell model. (Reprinted from D Chillura-Martino *et al* 1996 Neutron scattering characterization of polymerization mechanisms in supercritical CO_2 *J. Mol. Struct.* **383** with permission from Elsevier Science.)

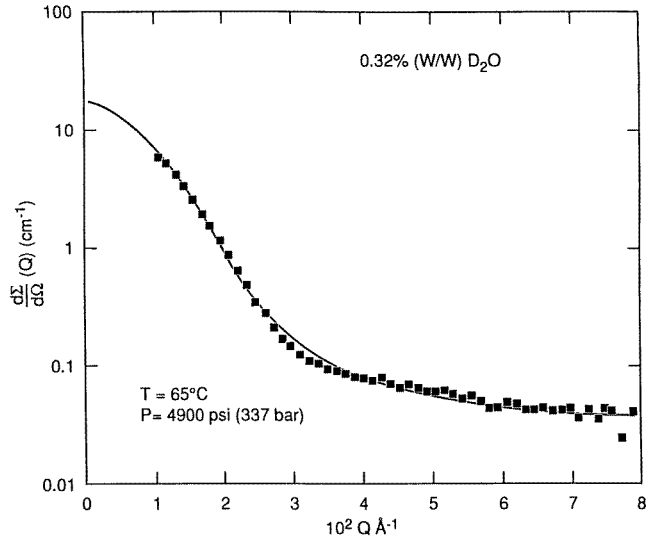

Figure 10. SANS data from 1.9% (w/v) PFOA-g-PEO graft copolymer in D_2O-saturated CO_2 compared to the polydisperse core–shell model. (Reprinted from D Chillura-Martino *et al* 1996 Neutron scattering characterization of polymerization mechanisms in supercritical CO_2 *J. Mol. Struct.* **383** with permission from Elsevier Science.)

Other SANS investigations of water-in-CO_2 microemulsions were undertaken by Eastoe and co-workers [23], who studied di-chain hydrocarbon–fluorocarbon surfactants that formed spherical droplets, which were modelled as a system of core–shell particles obeying a Schultz

distribution of radii (equation (6)). The mean core radius was ∼25 Å and the molar ratio of water/surfactant ∼33. The SANS signal was maximized by using D_2O to swell the micelle and, similarly, Zielinski and coworkers [22] studied D_2O-swollen microemulsions of ammonium perfluoropolether surfactants. As the D_2O concentration increased, the core radius increased from 20 to 35 Å and at constant water concentration the micellar structure was essentially independent of pressure. In both studies, the surfactant was shown to dissolve up to its own weight (∼2%) of water in CO_2 and the critical fluctuations or 'droplet clustering' increased as the pressure was reduced and the phase boundary was approached. Similarly, SANS measurements of the droplet size and interactions near the phase boundaries of water-in-propane microemulsions [27] based on the ionic surfactants bis(2-ethylhexyl)sulphosuccinate and didodecyldimethylammonium bromide were modelled by a core–shell model with a structure factor $S(Q)$ represented by the Ornstein–Zernike expression. The droplet radius (∼40 Å) was essentially independent of pressure, though in studies of the non-ionic ethylene (E) glycol-based surfactant $C_{12}E_5$, the core radius decreased from ∼70 Å to ∼54 Å, as the pressure decreased from 400 to 120 bar, thus demonstrating that the mechanisms of pressure induced phase transitions depended on the surfactant type [27].

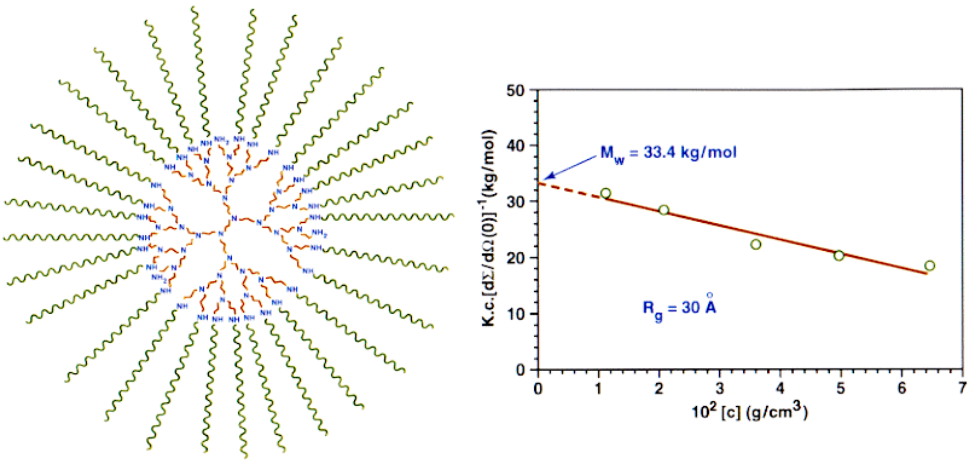

Figure 11. SAXS characterization of a fourth-generation hydrophilic dendrimer, functionalized with perfluoroether chains to generate a CO_2-soluble unimolecular micelle. (Reprinted with permission from *Nature* **389** 368. Copyright 1997 Macmillan Magazines Limited.)

These studies reflect the growing interest CO_2-soluble amphiphiles to provide havens for hydrophilic material in CO_2 and thus broaden the potential applications in separations and extraction processes [50]. The use of such highly CO_2-soluble amphiphiles may allow the operating pressure of novel extraction processes to be lowered closer to the point of economic viability. Similarly, CO_2-soluble dendritic molecules have been shown [10] to act as micelle-like entities, which are capable of solubilizing CO_2-insoluble materials (e.g. polar ionic species) in their cores. Dendrimers are well defined, highly branched polymers which form a range of guest–host systems. Figure 11 shows a schematic illustration of a fourth-generation hydrophilic dendrimer, functionalized with perfluoroether chains to generate a CO_2-soluble dendritic 'micelle'. SAXS data (figure 11) confirm that the molecular weight (33.4 kg mol^{-1}) and radius of gyration (30 Å) are consistent with the micelle containing only one molecule. Remarkably, the dendritic micelle can also transfer ionic species (e.g. a methyl orange polar dye) from aqueous solution into CO_2 without forming a water-in-oil microemulsion [10].

These experiments demonstrate that CO_2 modified with a surfactant can efficiently magnify the partitioning of CO_2-insoluble materials into a CO_2-rich phase. Thus, surfactant-modified CO_2 can be used to dramatically enhance the applicability of supercritical extractions to replace some of the large quantities of organic solvents used annually in cleaning and extraction applications and CO_2-based dry cleaning processes are already nearing commercialization [53].

4.2. Solubilization of polymers in CO_2

Surface active agents (surfactants), comprised of CO_2-phobic/CO_2-philic segments have recently been developed to emulsify CO_2-insoluble polymers. Controlled free radical polymerization methods have been employed to synthesize a series of diblock-copolymers, which possess amphiphilic character imparted by a 'CO_2-phobic' polystyrene block and a 'CO_2-philic' PFOA block [5, 54, 55]. In supercritical CO_2, these block-copolymers form micelles consisting of a lipophilic core of styrene and a CO_2-philic corona of the fluorinated acrylate segments [5, 9]. This is illustrated schematically in figure 12, which compares the formation of micelles in conventional oil-in-water systems with those in CO_2. It is well known that hydrophobic oil (O) may be solubilized in water (W) by coating the oil droplets with the hydrophilic (water-soluble) component of a detergent (figure 12). Much of the knowledge base established over the past 80 years for O/W and W/O emulsions may be carried over from aqueous surfactant behaviour to molecules that function as surfactants in CO_2.

The results are summarized in table 2 where the block-copolymers are referred to via the number average molecular weights of the blocks, $\langle M_n \rangle_{styrene}/\langle M_n \rangle_{FOA}$, as determined using ^{1}H NMR. Figure 13 illustrates the phenomenon of micelle formation, caused by the aggregation

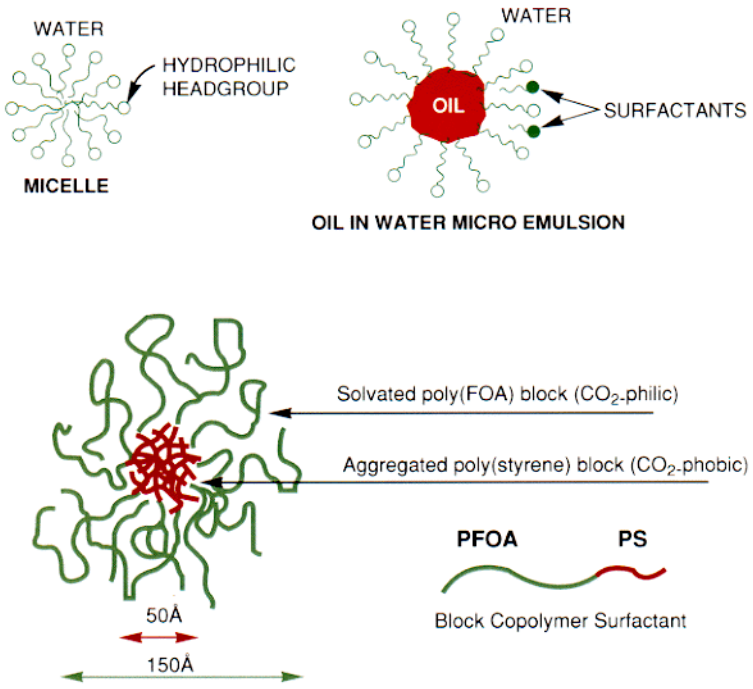

Figure 12. Schematic representation of colloidal aggregates in water and supercritical carbon dioxide.

Table 2. The size of core–shell micellar aggregates, for PS-b-PFOA in SC-CO_2 at 65 °C and 5 kpsi, as a function of size of the shell (corona) block length. Copolymer concentration was 4% w/v.

Copolymer	Aggregation No (N_{agg})	Z	R_1 (Å)	R_2 (Å)
3.7 k/16.6 k	7	10	27	85
3.7 k/27.5 k	11	8	30	80
3.7 k/40 k	7	8	27	89
3.7 k/61 k	6	8	26	100

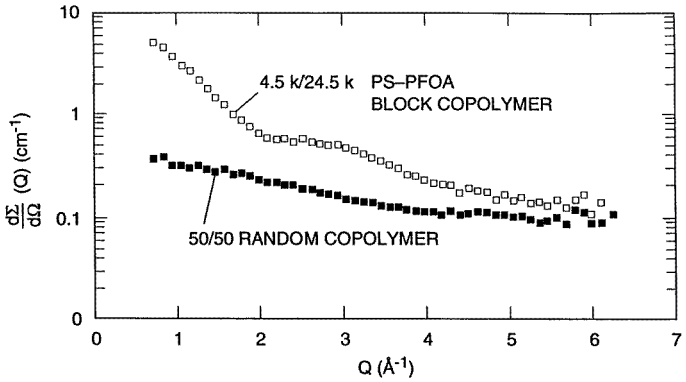

Figure 13. Comparison of SANS data for block and random copolymers.

of block-copolymers in solution, and compares the SANS cross-section of a diblock-copolymer solution with that of a random copolymer of similar molecular mass and overall molecular composition. The scattering from the diblock-copolymer is typical of a micellar fluid. The enhanced intensity indicates that the particle has a much higher molecular mass than the single molecule (unimer). The monotonic decay of the scattering from the random copolymer ($d\Sigma/d\Omega(Q) \sim Q^{-2}$) is typical of single molecules, whereas the existence of a subsidiary maximum is related to the spherical shape of the particle and these data were fitted to the polydisperse core–shell model (equations (2)–(5)). The three adjustable parameters were the average number of copolymer molecules per micelle, or aggregation number (N_{agg}); the breadth parameter (Z) in the Schultz distribution of micellar core diameters, which varies inversely with the variance of the distribution, and the number of CO_2 molecules per FOA monomer ($N(CO_2)$), which determines the degree of swelling of the shell. The radii R_1 and R_2 were calculated from the mass densities of the various components, and from the fitted parameters. The experiments were conducted at 65 °C and 344 bar (5000 psi) as a function of PFOA-block length, at constant PS-block length and copolymer concentration (4% w/v). A typical fit for the 4 k/17 k is shown in figure 14 and the SLDs of the solvent and core are $\rho_s = 2.1 \times 10^{10}$ cm^{-2} and $\rho_1 = 1.4 \times 10^{10}$ cm^{-2} respectively, assuming CO_2 and PS mass densities of 0.84 and 1.05 g cm^{-3}. As the shell is swollen with solvent, ρ_2 depends on ρ_s and ρ_{PFOA} (3.36×10^{10} cm^{-2}, estimated from the mass density of 1.7 g cm^{-3}), along with the volume fraction of the shell occupied by each component [9].

Table 2 lists the results from the fits to the core–shell polydisperse model, and shows that increasing the PFOA-block length by a factor of 3.5 has no effect on the polydispersity or the aggregation number (N_{agg}), which remains constant at ∼7 block-copolymer molecules per micelle. Thus N_{agg} seems to be relatively independent of the PFOA (corona) block length (table 2), as predicted by Halperin and coworkers [56], and, similarly, the inner radius (R_1)

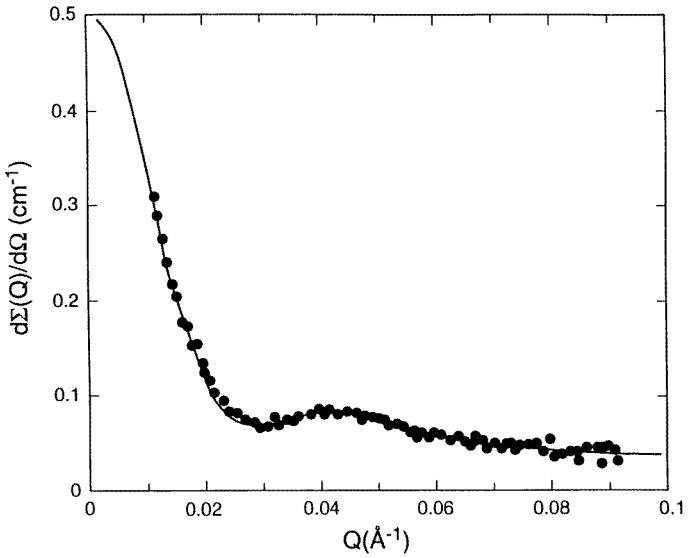

Figure 14. $d\Sigma/d\Omega$ versus Q for 3.7 k/16.6 k polystyrene–PFOA block-copolymer micelles and fit to core–shell model. (Reprinted with permission from 1997 *J. Appl. Crystallogr.* **30** 690.)

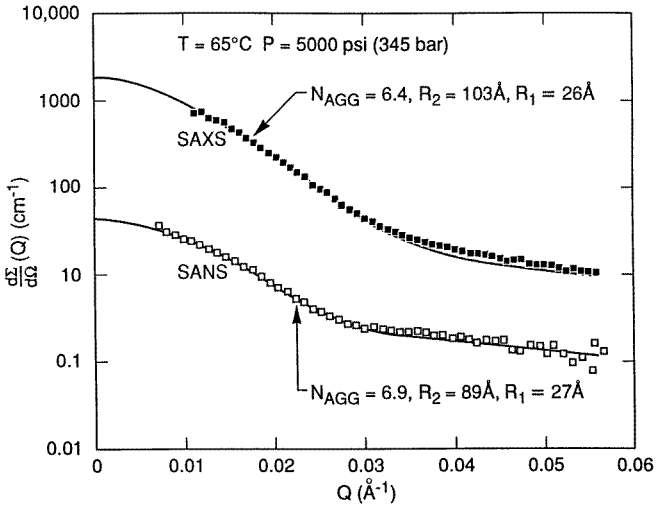

Figure 15. $d\Sigma/d\Omega$ against Q for independently calibrated SAXS (■) and SANS (□) data from 3.7 k/40 k PS-b-PFOA block-copolymer micelles in CO_2. (Reprinted with permission from 1997 *J. Appl. Crystallogr.* **30** 690.)

remains constant, as expected when the PS-block length is fixed. Figure 15 shows a comparison of the independently calibrated SAXS and SANS data taken from 3.7 k/40 k block-copolymer solutions at similar experimental conditions. The values of R_1 and N_{agg} resulting from model fits (figure 15) are virtually identical. This forms a useful cross-check on the validity of the methodology, as the contrast factors, and hence the weighting of the components of the structure, are quite different for SANS and SAXS.

4.3. Addition of CO_2-insoluble material

Polystyrene ($M_n = 0.5$ kg mol^{-1}) was added to the block-copolymer solutions, to study the solubilization of this material within the micelles. Separate concentration series were run for normal (PSH) and deuterated polystyrene (PSD). The isotopic difference should have little or no effect on the structure of the micellar fluid, yet a major effect on the intensity, as the SLD for PS increases by a factor of ∼6 on deuteration (to 6.48×10^{10} cm^{-2}). The core–shell model was modified, and a fourth adjustable parameter was introduced, to account for the fraction of oligomer solubilized in the core of the micelle (α). The results are listed in table 3, and indicate that virtually all of the added material is solubilized in the core ($\alpha \simeq 100\%$), independent of the PS concentration and isotopic content. The aggregation number, N_{agg}, increases and the distribution of aggregates becomes more monodisperse (increase in Z) with increase in the PS concentration. These trends are understandable, because as the core becomes larger with added oligomer, an increased number of fluorinated blocks are necessary to keep the aggregate in solution. Figure 16 shows how the forward SANS cross section (extrapolated to $Q = 0$) increases by over an order of magnitude as the particle size and aggregation number swell to accommodate the polystyrene solubilized in the core. Table 3 also shows values for R_1 and R_2, which were calculated from the adjusted model parameters. The agreement between the results from the two concentration series is noteworthy, considering the large change in the SLD of PS on deuteration, and confirms the reliability of the model and the results. It also indicates that isotope effects do not seriously perturb the SANS studies, as observed in bulk polymers, where they are only observed in high-molecular-weight (∼10^6) systems [12].

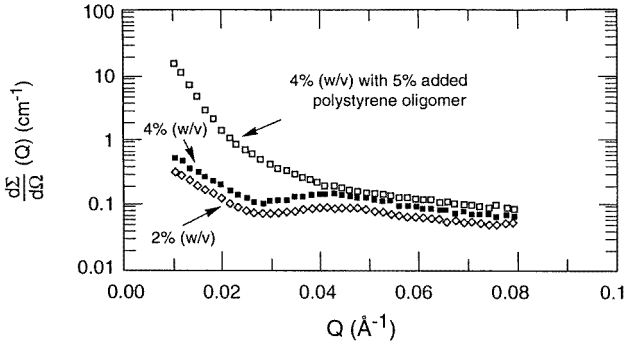

Figure 16. $d\Sigma/d\Omega$ versus Q for 3.7 k/16.6 k polystyrene–PFOA block-copolymer in supercritical CO_2 as a function of concentration (c) and added polystyrene oligomer (MW = 500).

4.4. Effect of solvent density on micellar morphology

Londono and co-workers [9] have compared the data from PS–PFOA copolymers at 40 °C, i.e. higher solvent density than the runs at 65 °C. The number of molecules per micelle (N_{agg}) decreases to about half of what was observed at 65 °C. This can be understood as an increase in surface area of block-copolymer in contact with the solvent, concomitant with the increase in solubility of the block-copolymer at higher density. The comparison also indicated an increase in polydispersity with respect to the results at 65 °C. It appears that the increase in solvent density has the effect of breaking apart a collection of aggregates of relatively low polydispersity (65 °C), into a collection of smaller aggregates of higher polydispersity. These results suggest the existence of a critical micellar density (CMD), which corresponds

Table 3. Effect of adding PSH or PSD; 3.7 k/40 k PS/PFOA @ 4% w/v; 5 kpsi and 65 °C.

% PSH (w/w)	% PSD (w/w)	Aggregation number (N_{agg})	Z	R_1 (Å)	R_2 (Å)	α (%)
0		7	8	27	88	0
2.7		8	8	32	90	99.8
	5.0	8	7.6	34	127	98.6
5.5		7.5	8.5	34	96	99.8
	12.5	11	11	48	114	99.4
13.0		11	13	46	129	99.8
	15.3	10	11	45	124	99.4
16.0		12	12	45	124	99.8
	16.6	14	12	51	118	99.1

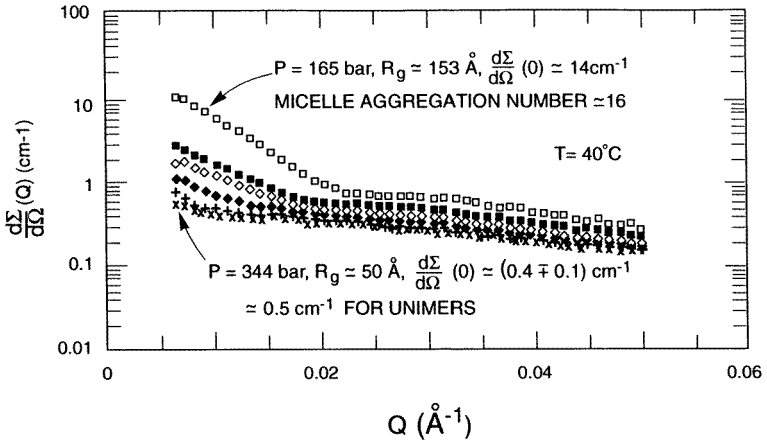

Figure 17. $d\Sigma/d\Omega(Q)$ for 8% (w/v) polyvinyl acetate-b-PFOA block-copolymers in CO_2. At high pressures, the scattering arises from single molecules; as the pressure is lowered, micelles form below a critical CO_2 density.

to the density of the solvent at which the micellar aggregates disappear [5]. Experiments on poly(vinyl acetate)-b-PFOA diblock-copolymers have confirmed this phenomenon [24], which is illustrated in figure 17. Thus, as the pressure is raised from 165 bar to 344 bar at constant concentration, the shapes and absolute magnitudes of the scattering curve change dramatically from curves characteristic of unimers ($d\Sigma/d\Omega(0) \sim 0.5\,cm^{-1}$; $R_g \sim 50$ Å), to those reflecting micellar aggregates ($d\Sigma/d\Omega(0) \sim 14\ cm^{-1}$; $R_g \sim 150$ Å). The latter data were modelled by the core–shell model, whereas the former were well fitted via a single-molecule form factor approximated via a Debye random coil [12].

$$[d\Sigma(Q)/d\Omega]_{RC} = 2\,d\Sigma/d\Omega(0)[(QR_g)^2 + \exp[(QR_g)^2] - 1]/(QR_g)^4. \quad (7)$$

The transition from random coils to aggregates is reasonably sharp, falling between 210 and 241 bar. It was found [24] that a fraction (∼25%) of the copolymers existed as single molecules (unimers), even at the lowest pressures. The aggregation number was virtually unaffected by changes in the CO_2 pressure, though the amount of CO_2 associated with the PVAc core triples as the pressure is increased from 165 bar and suddenly the aggregate breaks down when the pressure exceeds 206 bar as the solvent 'invades' the micelle. The sharpness of the transition suggests that the transformation is caused by the variation in density. The effect is analogous to that caused by changing the concentration of surfactants in aqueous media,

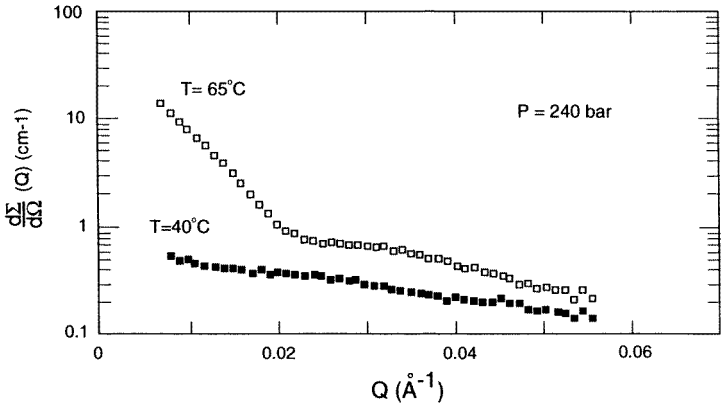

Figure 18. SANS cross-section for 8% (w/v) $4.4^k - b - 43.1^k$ PVAc–PFOA copolymer in supercritical CO_2. By changing the temperature, from 65 to 40 °C, the molecular aggregates (micelles) are dispersed into individual molecules (unimers).

where a micelle–unimer transition [14, 19] occurs at a critical micelle concentration (CMC). This phenomenon may also be observed in supercritical CO_2 [24], where a unimer to micelle transition occurs between 2% and 4% (w/v) at constant pressure and temperature. However, SCFs also display quite new and unique attributes. Thus, the solvent strength is a strong function of the CO_2 density and the system may be driven from an aggregated to a dispersed state simply by changing the pressure (figure 17). Similarly, changes in the temperature can dramatically change the solubility as illustrated in figure 18, which shows that the SANS cross-section changes by over an order of magnitude, thus reflecting the break-up of micellar aggregates into unimers as the temperature is reduced from 40 to 65 °C.

Poly(vinyl acetate)-b-PFOA diblock-copolymers in CO_2 have also been studied via LS by Zhao and Chu [32]. In addition to pressure-induced micellization, small amounts of anomalous large aggregates were observed around the critical phase separation pressure (∼225 bar), though the size of these assemblies (∼5000 Å) is beyond the resolution range of conventional SANS experiments. Otherwise, the aggregation numbers and CMCs were similar in the SANS and LS studies [24, 32]. The ability to create and disperse the micellar aggregates, coupled with the fact that CO_2-phobic materials can be solubilized within the micelles, makes the CMD an effect that may be of technological importance. The ability to understand and control such solubilization mechanisms is necessary for the development of CO_2-based technologies and scattering techniques have shown promise in delineating the underpinning science for such processes.

5. CO_2-based polymer processing

For both scientific and economic reasons, it has become increasingly difficult to commercialize completely new polymers. Because of this, industry has turned increasingly to combining (blending) existing polymers [57]. The ability to alter, in a tuneable fashion, the miscibility of polymer blends is therefore highly desirable, since it could expand the window of processability. While miscibility is achievable via the use of organic solvents, CO_2 represents an emerging, more benign alternative [58, 59] opportunity to accomplish this goal. Recent SANS experiments [60–62] have provided encouraging evidence that supercritical CO_2 can be used to shift the phase boundaries of polymer blends and block-copolymers. Watkins and co-workers have shown that phase-selective dilation has a dramatic effect on the location of the lower disorder–order transition in symmetric poly(styrene)-b-poly(*n*-butyl methacrylate)

copolymers [60]. Subsequently, it was demonstrated [61] that phase separation could be induced in a 50/50 homopolymer blend of polystyrene and polyvinylmethylether, for which the spinodal temperature at ambient pressure was 152 °C. Figure 19 shows that in the presence of CO_2, the system phase segregates at 40 °C, more than 110 °C below the ambient-pressure lower critical solution temperature.

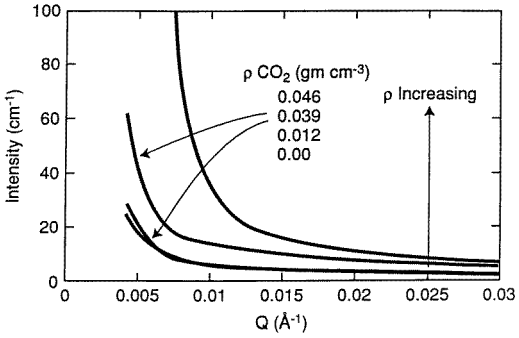

Figure 19. Density dependence of scattering profile for 50/50 PS/PVME blends at 40 °C.

Similarly Walker and co-workers [62] observed that the cloud points of low-molecular-weight mixtures of polystyrene and polyisoprene were depressed by as much as 28 °C by a CO_2 pressure of 150 bar. Complementary studies performed with N_2 were used to decouple the free-volume compression due to hydrostatic pressure from the plasticization efficacy of CO_2, which was shown to be responsible for the depression in the cloud point. This study provided evidence for enhanced polymer miscibility, though it is noteworthy that CO_2 can have the opposite effect (i.e. an increased range of immiscibility) in other blends [60, 61]. While the systematic study of such effects is only beginning, so generalizations cannot be made at this point, a trend that is consistent with the current investigations is that phase boundaries appear to be depressed (shifted to lower temperatures) in the presence of supercritical CO_2. Moreover these studies demonstrate that SANS can play an important role in understanding this interesting and potentially technologically useful effect.

6. Summary

SANS investigations of CO_2-soluble molecules at $T \sim 65$ °C and $P \sim 350$ bar indicate that CO_2 is either a 'good' solvent (PFOA), a theta solvent (HFPPO) or a 'poor' solvent (PDMS) and there is a close similarity between the behaviour of polymer molecules in organic solvents and in CO_2. In addition, it has verified the prediction that molecules adopt 'ideal' configurations, unperturbed by excluded volume effects, at a critical 'theta pressure' (P_θ) as they do in polymer solutions at the theta temperature (T_θ). For $P > P_\theta$ and $T > T_\theta$, the system exhibits a 'good solvent' domain, where the molecules expand beyond the unperturbed R_g, measured in the condensed state. For $T < T_\theta$ and $P < P_\theta$, the system enters the 'poor solvent' domain, though diverging concentration fluctuations prevent the chains from collapsing and allow them to maintain their unperturbed dimensions.

Studies of block-copolymer surfactants have shown that they form micellar aggregates when CO_2 is a preferential solvent for one of the blocks and that the micellar cores are capable of solubilizing CO_2-insoluble material. A transition from unimers to aggregates occurs as a function of pressure, thus demonstrating that solvent strength is a function of the solvent density.

The CMD and 'theta pressure' constitute new concepts in colloid and surface chemistry. The self-assembly of molecules in condensed phases is a ubiquitous phenomenon found in many biological structures, as well as in systems of interest to materials, colloid and surface science. The experiments described above indicate that neutron scattering has the potential to give the same level of microstructural insight into individual polymer molecules (unimers) and colloidal aggregates (micelles) in supercritical CO_2 that it has provided in the condensed state and in aqueous media. A unique attribute of SCFs is that the solvent strength is easily tunable with changes in the system density, offering unprecedented control over the solubility. Understanding the solubility mechanisms that enable polymer molecules to be dissolved and processed in SCFs provides the enabling science for new environmentally benign technologies, as well as for liquid–liquid extractions via the phase transfer of water-soluble substances from water into a surfactant-rich CO_2 phases.

Acknowledgments

The author wishes to thank Professor Sow-Hsin Chen (MIT) for his encouragement to write a review article on this subject. He also wishes to acknowledge his co-workers at Oak Ridge (J D Londono and Y B Melnichenko) and at the Universities of North Carolina (D E Betts, D A Canelas, J M DeSimone, J B McClain, E T Samulski) and Palermo (R Triolo), with whom he has collaborated in many of the studies cited. Figures 7 and 19 were provided by Professor J J Watkins (University of Massachusetts) and Dr J L Fulton (Pacific Northwest Laboratory) who also helped clarify the definitions of micelles, reverse (inverted) micelles and microemulsions. The research was supported by the Divisions of Advanced Energy Projects, Materials and Chemical Sciences, US Department of Energy under contract No DE-AC05-96OR22464 with Lockheed Martin Energy Research Corporation.

References

[1] McHugh M A and Krukonis V J 1986 *Supercritical Fluid Extraction* (Chapel Hill: University of North Carolina)
[2] Guan Z 1994 *PhD Thesis* (Chapel Hill: University of North Carolina)
[3] McClain J B, Londono J D, Romack T J, Canelas D P, Betts D E, Wignall G D, Samulski E T and DeSimone J M 1996 *J. Am. Chem. Soc.* **118** 917
[4] Chillura-Martino D *et al* 1996 *J. Mol. Struct.* **383** 3
[5] McClain J B, Londono J D, Chillura-Martino D, Triolo R, Betts D E, Canelas D A, Cochran H D, Samulski E T, DeSimone J M and Wignall G D 1996 *Science* **274** 2049
[6] DeSimone J M, Guan Z and Elsbernd C S 1992 *Science* **257** 945
[7] DeSimone J M, Maury E E, Menceloglu Y Z, McClain J B and Romack T R 1994 *Science* **265** 356
[8] Guan Z and DeSimone J M 1994 *Macromolecules* **27** 5527
[9] Londono J D *et al* 1997 *J. Appl. Crystallogr.* **30** 690
[10] Cooper A I, Londono J D, Wignall G D, McClain J B, Samulski E T, Lin J S, Dobrynin A, Rubinstein M, Frechet J M and DeSimone J M 1997 *Nature* **389** 368
[11] Wignall G D 1987 *Encyclopedia of Polymer Science and Engineering* ed M Grayson and J Kroschwitz (New York: Wiley)
[12] Wignall G D 1993 *Physical Properties of Polymers* ed J E Mark (Washington, DC: ACS)
[13] Hayter J B 1985 *Physics of Amphiphiles, Micelles, Vesicles and Microemulsions* ed V de Giorgio and M Corti (Amsterdam: North-Holland)
[14] Magid L J 1986 *Colloids Surf.* **19** 129
[15] Cotton J P, Decker D, Benoit H, Farnoux B, Higgins J S, Jannink G, Ober R, Picot C and des Cloizeaux J 1974 *Macromolecules* **7** 863
[16] Cotton J P, Decker D, Farnoux B and Jannink G 1972 *J. Chem. Phys.* **57** 290
[17] Daoud M, Cotton J P, Farnoux B, Jannink G, Sarma G, Benoit H, Duplessix R, Picot C and de Gennes P G 1975 *Macromolecules* **8** 804
[18] King J S, Boyer R, Ullman R and Wignall G D 1985 *Macromolecules* **18** 709
[19] Caponetti E and Triolo R 1990 *Adv. Colloid Interface Sci.* **32** 235

[20] Zielinski R G, Kaler E W and Paulaitis M E 1995 *J. Chem. Phys.* **99** 10 354
[21] Zielinski R G, Paulaitis M E and Kaler E W 1996 *J. Chem. Phys.* **100** 9465
[22] Zielinski R G, Kline S R, Kaler E W and Rostov N 1997 *Langmuir* **13** 3934
[23] Eastoe J, Bayazit Z, Martel S, Steytler D C and Heenan R K 1996 *Langmuir* **12** 1423
[24] Triolo R, Triolo F, Triolo A, Londono J D, Wignall G D, McClain J B, Betts D E, Canelas D A, DeSimone J M and Samulski E T *Langmuir* submitted
[25] Eastoe J and Steytler B H 1996 *Rutherford Appleton Laboratory ISIS Facility (UK) Annual Report* A301
[26] Kaler E W, Billman J F, Fulton J L and Smith R D 1991 *J. Phys. Chem.* **95** 458
[27] Eastoe J, Steytler D, Robinson B H and Heenan R K 1994 *J. Chem. Soc. Faraday Trans.* **90** 3121
[28] Zielinski R G, Paulaitis M E and Kaler E W 1996 *Rev. Sci. Instrum.* **67** 2612
[29] Londono J D, Shah V M, Wignall G D, Cochran H D and Bienkowski P R 1993 *J. Chem. Phys.* **99** 466
[30] Pfund D M, Zemanian T S, Linehan J C, Fulton J F and Yonker C R 1994 *J. Phys. Chem*. **98** 846
[31] Fulton J L, Pfund D M, McClain J B, Romack T J, Maury E E, Combes J R and Capel M 1995 *Langmuir* **11** 4241
[32] Zhou S and Chu B 1998 *Macromolecules* **31** 5300
[33] Zhou S, Chu B and Dhadwal H S *Rev. Sci. Instrum.* submitted
[34] Koehler W C 1986 *Physica* B **137** 320
[35] Wignall G D and Bates F S 1986 *J. Appl. Crystallogr.* **20** 28
[36] Hendricks R W 1978 *J. Appl. Phys.* **11** 15
[37] Wignall G D, Lin J S and Spooner S 1990 *J. Appl. Crystallogr.* **23** 241
[38] Russell T P, Lin J S, Spooner S and Wignall G D 1988 *J. Appl. Crystallogr.* **21** 629
[39] Carnahan N F, Quintero L, Pfund D M, Fulton J L, Smith R D, Capel M and Leontaritis K 1993 *Langmuir* **9** 2035
[40] Lindner P and Zemb T (eds) 1991 *Neutron, X-Ray and Light Scattering (North-Holland Delta Series)* (New York: Elsevier)
[41] Fujita H 1990 *Polymer Solutions* (Amsterdam: Elsevier) p 44
[42] Chu B, Ying Q and Grossman A 1995 *Macromolecules* **28** 180
[43] deGennes P G 1973 *Scaling Concepts in Polymer Physics* (New York: Cornell University Press Ithaca) ch 3
[44] Melnichenko Y B and Wignall G D 1997 *Phys. Rev. Lett.* **78** 686
[45] Melnichenko Y B, Wignall G D, Van Hook W A, Szydlowski J, Rebello L P and Wilczura H 1998 *Macromolecules* **31** 8436
[46] Melnichenko Y B, Kiran E, Wignall G D, Heath K D, Salaniwal S, Cochran H D and Stamm M *Phys. Rev. Lett.* submitted
[47] Kiran E and Sen Y L 1993 *Supercritical Fluid and Engineering Science (ACS Symp. Ser. 514)* ch 9
[48] Elworthy P H, Florence A T and McFarlane C B 1968 *Solubilization of Surface-Active Agents* (London: Chapman and Hall)
[49] Hayter J B and Penfold J 1981 *Mol. Phys.* **42** 109
[50] Beckman E J 1996 *Science* **271** 613
[51] Rouhi M 1996 *Chem. Eng. News* 5 February, p 8
[52] Johnston K P, Harrison K L, Clarke M J, Howdle S M, Heitz M P, Bright F V, Carlier C and Randolph T W 1996 *Science* **271** 624
[53] See http://www.micell.com
[54] Guan Z and DeSimone J M 1994 *Macromolecules* **27** 5527
[55] Canlelas D A, Betts D E and DeSimone J M 1996 *Macromolecules* **29** 2818
[56] Halperin A, Tirrell M and Lodge T P 1992 *Adv. Polym. Sci.* **100** 31
[57] Lohse D J 1986 *Polym. News* **12** 8
[58] Mawson S, Johnston K P, Betts D E, McClain J B and DeSimone J M 1997 *Macromolecules* **30** 71
[59] Mawson S, Kanakia S and Johnston K P 1997 *Polymer* **38** 2957
[60] Watkins J J, Brown G D, Pollard M A, Ramachandra-Rao V and Russell T P 1998 *Polym. Mater. Sci., Eng.* **78** 94
[61] Watkins J J, Brown G D, Pollard M A, Ramachandra-Rao V and Russell T P 1998 *Polym. Mat. Sci., Eng.* **79** 386
[62] Walker T A, Raghaven S R, Royer J R, Khan S A, Spontak R, Smith S D, Wignall G D and Melnichenko Y B *Macromolecules* submitted